Modelling the bronchial barrier in pulmonary drug delivery: a human bronchial epithelial cell line supplemented with human tracheal mucus

Xabi Murgia[a], Hanzey Yasar[a], Cristiane Carvalho-Wodarz[a], Brigitta Loretz[a], Sarah Gordon[a], Konrad Schwarzkopf[b], Ulrich Schaefer[c], and Claus-Michael Lehr[a,c*]

[a] Helmholtz Institute for Pharmaceutical Research Saarland (HIPS), Helmholtz Centre for Infection Research (HZI), Saarland University, 66123 Saarbrücken, Germany

[b] Department of Anesthesia and Intensive Care, Klinikum Saarbrücken, 66119 Saarbrücken, Germany

[c] Biopharmaceutics and Pharmaceutical Technology, Department of Pharmacy, Saarland University, 66123 Saarbrücken, Germany

* Corresponding author. E-Mail address: claus-michael.lehr@helmholtz-hzi.de

Key words: Cystic fibrosis, pulmonary mucus, epithelial drug delivery, nanoparticles

Graphical abstract

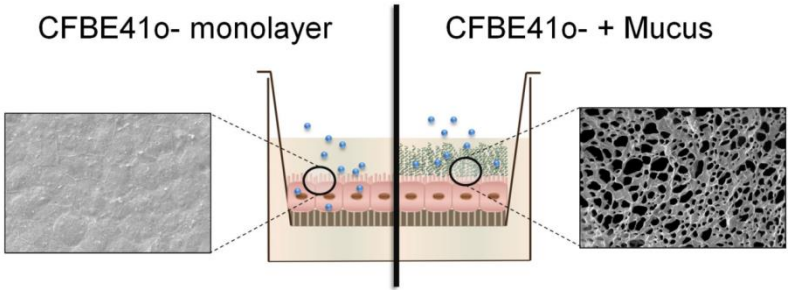

ABSTRACT

The airway epithelium together with the mucus layer coating it form a protective system that efficiently filters and removes potentially harmful particles contained in inhaled air. The same mechanism, however, serves to entrap particulate drug carriers, precluding their interaction with their target. The mucus barrier is often neglected in *in vitro* testing setups employed for the assessment of pulmonary drug delivery strategies. Therefore, our aim was to more accurately model the bronchial barrier, by developing an *in vitro* system comprising a tight epithelial cell layer which may be optionally supplemented with a layer of human tracheal mucus. To form the epithelium *in vitro*, we used the cystic fibrosis cell line CFBE41o-, which can be grown as monolayers on Transwell® supports, expressing tight junctions as well as relevant transport proteins. In contrast to the cell line Calu-3, however, CFBE41o- does not produce mucus. Therefore, native human mucus, obtained from tracheal tubes of patients undergoing elective surgery, was used as a supplement. The compatibility of CFBE41o- cells with the human mucus was addressed with the MTT assay, and confirmed by fluorescein diacetate/propidium iodide live/dead staining. Moreover, the CFBE41o- cells retained their epithelial barrier properties after being supplemented with mucus, as evidenced by the high trans-epithelial electrical resistance values (~1000 $\Omega*cm^2$) together with a continued low level of paracellular transport of sodium fluorescein. Fluorescently-labelled chitosan-coated PLGA nanoparticles (NP, ~168 nm) were used as a model drug delivery system to evaluate the suitability of this *in vitro* model for studying mucus permeation and cell uptake. Comparing CFBE41o- cell monolayers with and without mucus, resp., showed that the NP uptake was dramatically reduced in the presence of mucus. This model may therefore be used as a tool to study potential mucus interactions of aerosolized drugs, and more specifically NP-based drug delivery systems designed to exert their effect in the bronchial region.

1. INTRODUCTION

The conducting airways of the lungs are coated with a viscoelastic secretion, the pulmonary mucus, which moisturizes the inhaled air and acts as a filter for inhaled particles. In the healthy state, mucus is composed of water (95% w/w), glycoproteins (mucins, 2–5%), salts, non-mucin proteins, lipids, DNA, enzymes, cells and bacteria (1-3). The mucins are continuously secreted into the airway lumen by specialized secretory cells, and polymerize to form a mesh-like structure that is constantly being propelled out of the lungs by the ciliary beating of the airway epithelial cells - this creates a dynamic barrier termed as mucociliary clearance (4-6). In disease states such as asthma, chronic obstructive pulmonary disease (COPD), and in particular cystic fibrosis (CF) considerable changes in the mucus can occur, leading to mucus oversecretion and mucus thickening (7-10); this in turn can compromise the mucus clearance mechanism, providing optimal conditions for bacterial growth and chronic infection (11).

CF is a lethal genetic disease caused by a mutation of the CF transmembrane conductance regulator (CFTR). This results in numerous irregularities including an abnormal hydration of the airways, which leads to an impairment of the mucociliary machinery, recurrent infections, and eventually premature death (11). The clinical management of CF focuses primarily on improving the mucociliary clearance and combating chronic infections rather than targeting the primary cause, namely correcting the genetic disease. The potential of nanomedicine to improve the efficiency of gene-therapy in such diseases by using nanoparticle (NP)-based drug delivery systems is considerable, as evidenced by efficient transfection of cell-based *in vitro* models including the CF cell line CFBE41o- (12-14). This cell line was generated by transformation of CF airway cells with the SV40 virus and is homozygous for the most common CF mutation, the F508-CFTR mutation. Of particular interest to pharmaceutical research is the ability of this cell

line to express tight-junction proteins such as claudin-1, ZO-1, and occludin (15), which confer on CFBE41o- monolayers significant epithelial barrier properties evidenced by high transepithelial electrical resistance (TEER) values (15-18). This cell line also expresses a number of proteins relevant for pulmonary drug transport, including P-glycoprotein (P-gp), lung resistance-related P protein (LRP), and caveolin-1 (15). Unfortunately, unlike other pulmonary cell lines such as Calu-3, which are able to secret mucus (19-21), the CFBE41o- cell line lacks the capacity to synthesize and secret mucus onto the cell monolayer - a key feature that must be taken into account in the context of airway research. In particular, with regard to the use of NP-based drug delivery systems to treat bronchial diseases, our work and that of others has previously shown that particles with a diameter above 200 nm are almost exclusively trapped within the pulmonary mucus (3, 22, 23). Moreover, with a net negative charge under physiological conditions (24, 25), mucus represents a significant barrier to positively charged nanocarriers (21, 26), which are often used in the context of nucleic acid delivery for transfection purposes (27-29).

Therefore, in the present study we explored the possibility to develop an *in vitro* model of the airways composed of a CFBE41o- cell layer coated with human tracheal mucus. Our aim was to take a step forward in accurately mimicking the scenario within the CF lung, by utilizing the positive features of the CFBE41o- cell line in the context of pharmaceutical research and further introducing mucus as a key non-cellular barrier of the airways. For this purpose we cultured CFBE41o- cells in Transwell® supports and added a layer of human tracheal mucus on top of the cell monolayer, creating an air-mucus interface. The biocompatibility of CFBE41o- cells with the human tracheal mucus was investigated by measurement of epithelial barrier properties upon incubation with the exogenous mucus. Ultimately, as a proof-of-concept validation of the implemented *in vitro* model, we produced chitosan-poly(d,l-lactide-co-glycolide; PLGA)

nanoparticles and determined the effect of the mucus layer on the cellular uptake of such particles.

2. METHODS

2.1 Human mucus sample collection

Undiluted human tracheal mucus samples were collected by the endotracheal tube method (3, 30, 31), after obtaining informed consent from patients and in compliance with a protocol approved by the Ethics Commission of The Chamber of Medicine Doctors of the Saarland (file number 19/15). The tracheal tube of patients undergoing elective surgery with general anesthesia, non-related to pulmonary conditions, was collected after surgery. The distal portion of the tracheal tube (5-10 cm), including the balloon, was cut and placed in a 50 ml centrifuge tube. The mucus of each tracheal tube was collected by centrifuging the samples at 190 g for 30 s. Samples with visible blood contamination were excluded from the analysis. Mucus samples were stored at -20 °C until further use. In total 16 mucus samples from independent patients were used in this study. The mean age of the patients was 56.8 ± 4.8 years, the male: female ratio was 12:4, and 6 out of 16 patients were smokers.

2.2 Freeze-dried Mucus disk preparation

Mucus samples frozen and stored at -20°C were thawed gradually and allowed to reach room temperature. Thereafter, single mucus drops with an approximate weight of 30-40 mg (34.17 ± 1.82 mg, n=45 mucus drops) were placed over a Teflon® surface and spread over delineated circular surfaces of 1.12 cm^2. The samples were then placed into an autoclavable sealing bag, stored at -80 °C for 4 h, and ultimately, freeze-dried overnight (Alpha 2-4 LSC, Christ, Germany). After completion of the preset freeze-drying program, the bag containing the mucus disks (1.7 ± 0.1 mg estimated solid content, for an estimated water content of 95%) was

immediately sealed and stored in a dry atmosphere at room temperature until further use. Five different batches with 14-20 mucus disks per batch were used in this study.

2.3 Mucus Characterization

2.3.1 Mucus bulk rheology

Experiments were conducted on an Anton-Paar MCR 102 rheometer (Graz, Austria) equipped with cone-plate geometry (diameter: 25 mm, cone angle: 2°) at room temperature. Strain amplitude (γ) sweeps were performed at a frequency of 1 Hz in the range of 0.1-10%. Frequency (ω) dependency of the storage modulus G' and the loss modulus G'' was measured in the range between 0.1 and 40 rad/s at a strain amplitude of 1%.

In the first set of experiments native undiluted tracheal mucus samples were gradually thawed and allowed to reach room temperature. Thereafter, an approximate volume of 150 µl of mucus was placed in the rheometer and the aforementioned protocol was conducted. In the second set of experiments previously freeze-dried and rehydrated mucus samples were analyzed. Mucus samples contained in 1.5 ml Eppendorf tubes were allowed to equilibrate to room temperature and weighed using a precision balance (CPA 224S, Sartorius, Göttingen, Germany). Afterwards, the samples were stored at -80 °C for 4 h followed by overnight freeze-drying (Alpha 2-4 LSC, Christ, Osterode am Harz, Germany). The freeze-dried (solid) content of the samples was weighed again to determine the water content of mucus. Mucus samples were then re-hydrated with exactly the same volume of sublimed water (Milli-Q water, Advantage A10, Merck Millipore, Billerica, MA), and were allowed to mix in a 360° multi-rotator (PTR-35, Grant instruments, UK) for at least two hours at room temperature. Thereafter, re-hydrated mucus samples were placed in the rheometer to perform the measurements as described above.

2.3.2 Scanning electron microscopy

The structure of pulmonary mucus was imaged by means of scanning electron microscopy (SEM). Human tracheal mucus samples were gradually thawed and spread over the surface of a SEM-imaging carbon disk. The mucus was freeze-dried *in situ* following the freeze-drying protocol as in section 2.2. Freeze-dried mucus samples were gold-sputtered (QUORUM Q150R ES, Gala Instrumente, Germany) and then transferred to the SEM (EVO HD15, Zeiss, Germany) for imaging.

In order to image the CFBE41o- cell monolayer and the combined model comprising the cell monolayer and the overlying mucus, the cells were seeded onto Transwell® permeable supports and were cultured until a confluent monolayer was reached (see section 2.4). The day before the SEM fixation the apical culture medium was removed and a mucus disk together with 100 µl of fresh medium were added to the apical compartment, creating an air mucus interface. The cells with the mucus disks in place were incubated for 24 h at 37 °C, 5% CO_2, in a horizontal shaker. After incubation the basolateral medium was aspirated and fixation was performed by adding 1 ml of glutaraldehyde (Sigma) 3%in PBS to the basolateral compartment for 2 h. Subsequently, dehydration was carried out through a graded series of ethanol (30–100%, 10 min each). In the final step 150 µl of hexamethyldisilazane (Fluka) were added to the apical compartment. The filter of the Transwells® was then cut with a scalpel and mounted onto SEM-stacks. Samples were further sputtered with gold and transferred to the electron microscope.

2.4 Cell Culture of CFBE41o-

CFBE41o- cells were a kind gift of Dr. Dieter C. Gruenert (University of California, San Francisco, CA, USA). Passages 78 to 90 were used in this study. Cells were passaged on a weekly basis (0.2 x 10^6 cells in a T75 flask) and grown in minimum essential medium (MEM,

Gibco) supplemented with 10% fetal calf serum (FCS, Lonza), 5% non-essential amino acids (NEAA 100x, Gibco), 0.54 mg/ml of D-(+)-glucose (Sigma), and 100 µg/ml streptomycin and 100 U/ml penicillin, at 37 °C in a 5% CO_2 incubator. For experimental purposes cells were seeded onto Transwell® permeable supports (3640, Insert diameter 12 mm, growth area 1.12 cm^2, pore size 0.4 µm; Corning, Wiesbaden, Germany) at a density of 1.5×10^5 cells/cm^2 and grown under submerged conditions with apical/basolateral fluid volumes of 500 µl/1100 µl, respectively. The culture medium was replaced every 2-3 days.

2.5 Nanoparticle preparation and characterization

PLGA (50:50; Resomer RG 503H) was purchased from Evonik Industries AG (Darmstadt, Germany); ultrapure chitosan chloride salt (Protasan UP CL113) was obtained from FMC Biopolymer AS NovaMatrix (Sandvika, Norway). Polyvinyl alcohol (PVA) Mowiol®4-88 was purchased from Sigma-Aldrich (Germany); the lipophilic fluorescent dye 1,1'-dioctadecyl-3,3,3',3'-tetramethylindodicarbocyanine perchlorate (DiD) was obtained from Thermofisher Scientific (Oregon, USA). Ethyl acetate was purchased from Sigma-Aldrich (Germany), and purified water was produced freshly by a Milli-Q water purification system (Merck Millipore, Billerica, MA).

Drug free, DiD-labeled chitosan-PLGA NPs were used as a model drug delivery system to evaluate the uptake behavior on CFBE41o- cell monolayers with and without mucus. Such NPs were prepared by using a modified double-emulsion method according to Mittal *et al.* (33). Briefly, a 0.2% w/v chitosan solution was first prepared by dissolving Protasan UP CL113 in a 2% w/v PVA solution. A 50 mg amount of PLGA was dissolved in 2 ml ethyl acetate and equilibrated with 15 µg/20 µl of DiD ethanolic solution under continuous stirring for 1 h at room temperature. A 400 µl volume of water was then added to the PLGA organic phase and sonicated

with ultrasound (Branson Ultrasonic Corporation, USA) at 20% amplitude for 20 s to allow the primary emulsion to form. Immediately afterwards, the PVA chitosan solution was applied to the primary emulsion and sonicated using the same settings, leading to the formation of a w/o/w emulsion. Milli-Q water was added dropwise to the w/o/w emulsion to allow for the evaporation of the organic solvent. The resulting chitosan coated PLGA NPs were purified by centrifugation at 15 000 g for 15 min and washed once with milli-Q water to remove any excess free dye. The size, polydispersity index (PDI) and ζ-potential of the DiD labeled chitosan-PLGA NPs were characterized using a Zetasizer Nano (Malvern Instruments, Malvern, UK). The morphological appearance of the carrier system was visualized using Transmission Electron Microscopy (TEM, JEM 2011, JEOL) and further with SEM (EVO HD15, Zeiss, Germany). Prior to the SEM measurements, NPs were put onto a carbon disc and gold-sputtered. In order to improve the contrast of the TEM images, NPs were further stained with 0.5% w/v phosphotungstic acid (Sigma).

2.6 Cytotoxicity assays

2.6.1 MTT assay

CFBE41o- cells were seeded in 96 well plates at a density of 20 000 cells per well and grown for 4 days. Cells were then washed twice with Hank's balanced salt solution (HBSS, Gibco) buffer, and 200 µl of fresh culture medium together with a freeze-dried mucus disk were added to the test wells. The cells were incubated for 24 h at 37 °C and 5% CO_2 in a horizontal shaker. Cells incubated with cell culture medium only served as positive controls (100% viability) and cells incubated with Triton-X 1% (Sigma) served as negative controls (0% viability). Following incubation, the mucus was removed by aspiration and the cells were washed twice with HBSS buffer. A 200 µl volume of the tetrazolium dye MTT (5 mg/ml) was added to each well, followed by 4 h incubation at 37 °C, 5% CO_2, in a horizontal shaker. Formed formazan crystals were then

solubilized by adding 200 µl of dimethyl sulfoxide (DMSO, Sigma). The absorbance of each well at 560 nm was measured with a plate reader (Infinite M200 Pro, TECAN), and the percentage of viable cells in each well was calculated as previously described (32).

2.6.2 Live/dead staining with fluorescein diacetate (FDA) and propidium iodide (PI)

CFBE41o- cells were seeded onto Transwell® permeable supports as described in 2.4 and were cultured for at least 10 days under submerged conditions. Live cells can take up and convert the non-fluorescent FDA into its fluorescent product fluorescein by means of cytosolic esterases, whereas PI cannot cross the membrane of viable cells but will stain the nuclei of non-viable cells by intercalating with the double helix DNA. Approximately 24 h before live/dead staining the apical medium was removed from each culture well, and a mucus disk together with 100 µl of fresh culture medium were added to apical compartments. The cells with the mucus disks in place were incubated for 24 h at 37 °C and 5% CO2 in a horizontal shaker. After 24 h, the mucus disks had dissolved creating an air-mucus interface in the apical compartment of each Transwell®. To proceed with the live/dead staining, medium was aspirated from mucus-containing apical compartments which were then washed twice with fresh medium. The cells were allowed to equilibrate for 30 min with 500 µl of freshly added cell culture medium, before this was replaced by 500 µl of the working solution of the FDA/PI live/dead stain (Sigma). The working solution itself was prepared in a 5 ml volume by adding 20 µl of FDA (5 mg/ml in acetone) and 100 µl of PI (2 mg/ml in PBS) to 4.88 ml of Phosphate-buffered saline (PBS, pH 7.4). The cells were incubated with the working solution for 5 min at room temperature, in the dark. The apical compartment of each well was then washed twice with cold PBS and the culture plate immediately transferred to a confocal laser scanning microscope (Leica TCS SP 8; Leica, Mannheim, Germany). Images of cell monolayers were acquired at 1024×1024 resolution, using

either a 25x water immersion (Fluotar VISIR 25x/0.95) or a 63x water immersion objective (HC APO CS2 63x/1.20). Image analysis was performed using LAS X software (Leica Application Suite X; Leica, Mannheim, Germany). Non-stained cells were used to preset the initial confocal settings. Cells that were not exposed to mucus served as positive controls and cells incubated with Triton-X 1% served as negative controls.

2.7 Functional mucosal barrier property assays

2.7.1 Evolution of TEER values of CFBE41o- cells cultured under submerged conditions

CFBE41o- cells were seeded onto Transwells® and grown under submerged conditions. TEER values were measured every 2-3 days for three weeks with an epithelial voltohmmeter equipped with STX2 chopstick manual electrodes (EVOM, World Precision Instruments, USA). A sharp increase in TEER values is associated with a confluent cell monolayer and the development of tight-junctions between neighboring cells. The raw TEER values were corrected according to the background resistance value of the Transwell® filter itself, and the growth area of the filter (1.12 cm^2).

2.7.2 TEER measurements with and without mucus incubation

CFBE41o- cells were seeded onto Transwell® permeable supports as described in 2.4 and were cultured for at least 10 days under submerged conditions. The apical medium was aspirated and a mucus disk together with 100 µl of fresh medium was added to the apical compartment. The cells with the mucus disks in place were incubated for 24 h at 37 °C and 5% CO2, in a horizontal shaker. The next day, the mucus-containing apical compartment was aspirated, washed twice with fresh culture medium, and the cells were allowed to equilibrate for 30 min with 500 µl of

freshly added cell culture medium in the apical compartment. Thereafter, TEER values were measured. Cells not exposed to mucus served as controls.

2.7.3 Permeability of sodium fluorescein

CFBE41o- cells were seeded onto Transwell® permeable supports as described in 2.4 and were cultured under submerged conditions for 7 days (the time point at which CFBE41o- cells displayed the highest epithelial barrier properties, according to TEER measurements). Apical compartments were then washed with Krebs-Ringer buffer (KRB) (NaCl 142.03 mM, KCl 2.95 mM, K2HPO4*3H2O 1.49 mM, HEPES 10.07 mM, D-glucose 4.00 mM, MgCl2*6H2O 1.18 mM, CaCl2*2H2O 4.22 mM; pH 7.4) and a mucus disk together with 100 µl of KRB buffer were added, and incubated for 4 h. Control wells incubated with just 100 µl of KRB served as controls. After the incubation, the basolateral culture medium was aspirated and the cells were washed twice with KRB. A volume of 1.5 ml of fresh KRB was then added to the basolateral compartment. The transport study was initiated by adding 500 µl of sodium fluorescein (10 µg/ml) to the apical (donor) compartment. The paracellular transport of sodium fluorescein was determined by sampling 200 µl from the basolateral (acceptor) compartment at various time points (0, 5, 15, 30, 60, 90 and 120 min). The withdrawn basolateral volume at each sampling point was replaced by the same volume of fresh pre-warmed KRB buffer. Throughout the experiment the cells were incubated at 37 °C and 5% CO2 on a horizontal shaker. The permeated amount of sodium fluorescein at each time-point was assessed by means of fluorescence intensity using a plate reader (Infinite M200PRO, Tecan, Germany) at excitation and emission wavelengths of 488 and 530 nm respectively. The apparent permeability coefficient (P_{app}) was then calculated by applying the formula:

$$P_{app} = (dQ/dt) / (A*C_0) \quad (1)$$

where dQ/dt is the flux (µg/s of permeated sodium fluorescein, obtained from the slope of the linear region of each individual permeation profile), A the area of the filter insert (1.12 cm^2), and C_0 the initial donor concentration of sodium fluorescein. C_0 was assumed to be 8.33 µg/ml in all wells, considering that 500 µl of sodium fluorescein (10 µg/ml) were added to a pre-existing apical volume of 100 µl.

2.7.4 Permeability through mucus and cellular uptake of nanoparticles

CFBE41o- cells were seeded onto Transwell® permeable supports as described in 2.4 and were cultured under submerged conditions for at least 10 days. The apical medium was then aspirated and a mucus disk with 100 µl of medium was added to the apical compartment followed by a 24 h incubation to allow for disk dissolution and creation of an air-mucus interface. Volumes of 400 µl of the DiD-labeled chitosan-PLGA NPs were then added to the apical compartment at a concentration of 40 µg/ml and were incubated for an additional 24 h. After incubation, the apical compartment, including the mucus, was aspirated and the cells were washed twice with PBS. In the following step 100 µl of wheat germ agglutinin (10 µg/ml, Vector Labs, CA, USA) were added to the apical compartment in order to stain the cell membrane. The cells were again washed twice with PBS and fixed with 3% paraformaldehyde (PFA, 15710-5, Electron Microscopy Science, USA) in PBS, for 30 min, at room temperature. After fixation cells were washed twice with PBS and then 200 µl of 4',6-diamidino-2-phenylindole (0.1 µg/ml, DAPI, Life Technologies, Darmstadt, Germany) were added to the apical compartment (10-15 min), followed by two further washes with PBS. Cell monolayers underwent a total of 8 PBS washes, which removed almost all the mucus as well as extracellular NPs. Finally, the filter membrane of each Transwell® insert was cut out with a scalpel and mounted on a glass slide with mounting medium (DAKO, Product No 85 5302380-2, USA). Mounted samples were stored at 4° C until

analysis by confocal laser scanning microscopy (Leica TCS SP 8; Leica, Mannheim, Germany). Images were acquired at 1024×1024 resolution, using a 63x water immersion objective (HC APO CS2 63x/1.20). Image analysis was performed using LAS X software (Leica Application Suite X; Leica, Mannheim, Germany).

2.8 Statistical analysis

All values are given as mean ± standard error of the mean (SE). Statistical analysis was performed with the SPSS statistics software (IBM, Germany). The storage and loss moduli of the native versus the freeze-dried and re-suspended mucus were compared using one-way ANOVA. The TEER values before and after mucus addition, P_{app} values, and permeated amounts of sodium fluorescein were compared using an independent samples t-test with Levene's test for equality of variances. A $P < 0.05$ was accepted as significant.

3. RESULTS AND DISCUSSION

3.1 CFBE41o- monolayers display high TEER values already after 5 days in submerged culture

CFBE41o- cells grown under submerged conditions displayed high TEER values within just 5 days of being seeded on Transwell® supports (Figure 1). The TEER values peaked between days 5-9 with values above 1500 Ω*cm^2. TEER values stabilized after day 10 (with the exception of a slight decrease between days 10-15) at approximately 1000 Ω*cm^2, indicating optimal epithelial barrier properties within this time period.

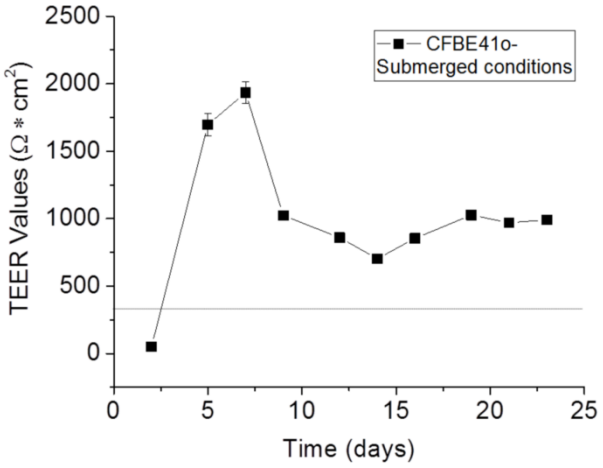

Figure 1. Time-course of TEER values measured for the CFBE41o- cell line cultured under submerged conditions. The horizontal line at 300 Ω*cm^2 indicates the threshold values deemed to indicate the presence of a tight barrier. The mean±SE for n=25, from 4 independent experiments are shown.

The noted TEER values are in line with previous studies and suggest the expression of functional tight junctions already within a few days of cell seeding on Transwell® membranes (15, 16). Equivalent bioelectric properties have been also described for other bronchial cell lines grown under submerged conditions such as 16HBE14o- cells, and the widely used Calu-3 cell

line (33-35). The Calu-3 cell line can secrete mucus, provided that cells are cultured at the air-liquid interface (20, 21). However, growing Calu-3 cells under this condition significantly decreases the TEER values (19, 36) and significantly increases the culture time needed to achieve both a tight epithelial barrier ($\geq 300\ \Omega*cm^2$) and a confluent mucus layer on top of the cells (20, 21). The TEER values of CFBE41o- cells are similarly low when cultured at the air-liquid interface (15), bordering on the threshold values deemed to indicate the presence of a tight barrier. In order to develop a relevant model that mimics the CF airway for pharmaceutical testing purposes, we therefore sought to combine the optimal epithelial barrier properties displayed by the CFBE41o- cell line grown under submerged conditions with the option to either add, or not to add, a supplementary human mucus layer.

3.2 In vitro model concept

The concept of the novel *in vitro* model involves growing CFBE41o- cells in Transwell® supports under submerged conditions until the monolayer develops optimal barrier properties. At this time-point the overlying culture medium is removed and the apical compartment is supplemented with freeze-dried human mucus in combination with a minimal volume of medium, creating an air-mucus interface. The human tracheal mucus samples obtained for the present work were initially nonsterile and highly elastic. Mucus samples are difficult to manipulate, precluding the possibility of pipetting precise mucus volumes or efficiently distributing mucus over a cell monolayer without damaging it. To overcome this limitation, we found a feasible alternative to freeze-dry small amounts of mucus in order to form thin disks, which could then be placed onto the cell monolayers and re-hydrated with a minimal amount of culture medium. Moreover, we speculate that the freeze-drying process may have accounted for a reduction in the microbial load of the exogenous human material.

3.3 Freeze-dried, re-suspended tracheal mucus show similar rheological properties to undiluted native mucus

The rheological properties of native undiluted mucus were compared to those of mucus samples that had undergone freeze-drying and subsequent re-hydration. With regard to the undiluted native tracheal mucus, in the tested strain range (0.1 to 10%) airway mucus was within the viscoelastic linear range (Figure 2A, black symbols). A strain of 1% was therefore chosen to determine the frequency dependence of the viscoelastic moduli. In the tested frequencies (0.1 to 40 rad/s) G' dominated over G'' in all the three decades of frequencies tested (Figure 2B, black symbols). These rheological properties are characteristic of cross-linked gels and are in line with previous studies reporting on the bulk rheological behavior of airway mucus (3, 10, 30). The G''/G' ratio of mucus determined at 1 rad/s represents a frequency value that is often used in mucus rheology to approximate the low velocities of mucociliary clearance (30, 31, 37). Materials with a ratio ranging between $0 \leq G''/G' \leq 1$ are classified as viscoelastic solids. The G''/G' ratio achieved here for the native tracheal mucus shows a mean value of 0.27±0.01, in good agreement with the values reported by Schuster *et al.* and Rubin *et al.* in which a G''/G' of 0.30 and 0.28 were respectively determined for airway mucus samples collected by the same method as employed in the current work (3, 31).

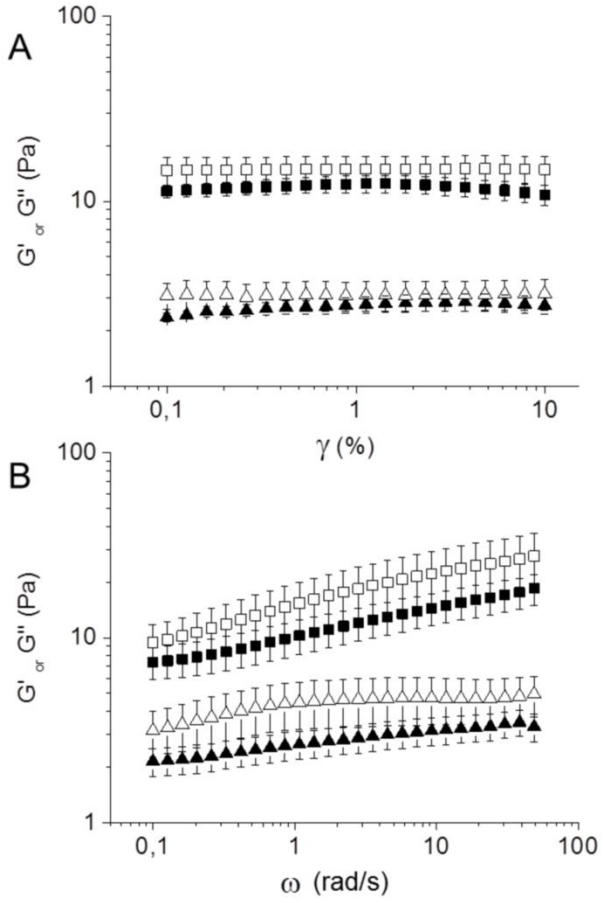

Figure 2. Bulk rheology of native human tracheal mucus (solid symbols) compared to native airway mucus which was freeze-dried and re-suspended (open symbols). (A) Strain (γ)-dependent viscous (G'', triangles) and elastic (G', squares) moduli from 0.1 to 10% strain at a frequency of 6.28 rad/s (1 Hz). (B) Frequency-dependent viscous (G'', triangles) and elastic (G', squares) moduli from 0.1 to 50 rad/s at 1% strain. The mean±SE for n=5 are shown.

Since our aim was to implement a mucus layer on top of the CFBE41o- cell monolayer using freeze-dried tracheal mucus, we investigated whether, upon re-hydration, the freeze-dried mucus would partially or completely recover the viscoelastic properties shown by the native material.

The water percentage of the mucus samples was 95.79 ± 0.62%, being the percentage of solid content of 4.20 ± 0.62. After re-hydration with exactly the same volume of sublimed water and 2 h

of mixing in a 360° rotator, the freeze-dried mucus displayed very similar viscoelastic properties as the undiluted human mucus, with no statistical difference between the elastic or viscous moduli at any of the strains or frequencies tested. As with the native material, G' exceeded G'' in both the amplitude and the frequency sweep test (Figure 2, white symbols). The viscoelastic moduli were slightly, but not significantly, higher in the case of the freeze-dried and re-hydrated mucus in comparison to the native material. The mean G''/G' ratio at 1 rad/s demonstrated a mean value of 0.29 ± 0.01, which confirms that intermolecular cross-linking and the characteristic mucus viscoelastic behavior were recovered after re-hydration.

3.4 CFBE41o- cells remain viable and retain their barrier properties after addition of external human freeze-dried mucus

The primary concern of adding an exogenous mucus to the CFBE41o- monolayers was a potential adverse effect that the human-derived tracheal mucus could exert on the cells. Previous studies attempting to implement exogenous mucus onto cell monolayers, had shown a clear disruption of the epithelial barrier properties and even some cytotoxicity (38, 39). Boegh *et al.* found a significant barrier disruption after incubating Caco-2 cells with native porcine intestinal mucus, as evidenced by the dramatic decrease in TEER values (38), whereas Teubl *et al*. reported a reduced viability of the oral epithelial cell line TR146 after a 24 hour incubation with mucins derived from bovine submaxillary glands (39). We hypothesized that due to the common human origin of both the CFBE41o- cells and the tracheal mucus, the cells and the mucus would be better compatible. To assess any potential toxic effects that the exogenous freeze-dried mucus could exert on the cells, the MTT assay was performed on proliferating CFBE41o- cells. However, after 24 hours of incubating the cells with mucus the viability was slightly higher than

in untreated control cells, suggesting even a positive effect of human mucus on the human-derived CFBE41o-cells under such conditions (Figure 3A).

In a subsequent step we sought to confirm the cell viability of CFBE41o- monolayers that were allowed to differentiate and to develop tight junctions in Transwell® using the so called live dead staining: in the case that cells are alive, the diffusion and subsequent esterase-mediated hydrolysis of the non-fluorescent dye FDA to the fluorescent product fluorescein will occur. In the case that cells are dead, PI will bind to DNA within the nuclei of cells in which the cell membrane is disrupted (Figure 3B). After staining with the working solution of FDA/PI we observed tightly packed CFBE41o- cells in confluent monolayers emitting high fluorescence intensity in the fluorescein detection range (Figure 3C, D, and E), confirming the high cell viability previously observed in proliferating cells with the MTT assay.

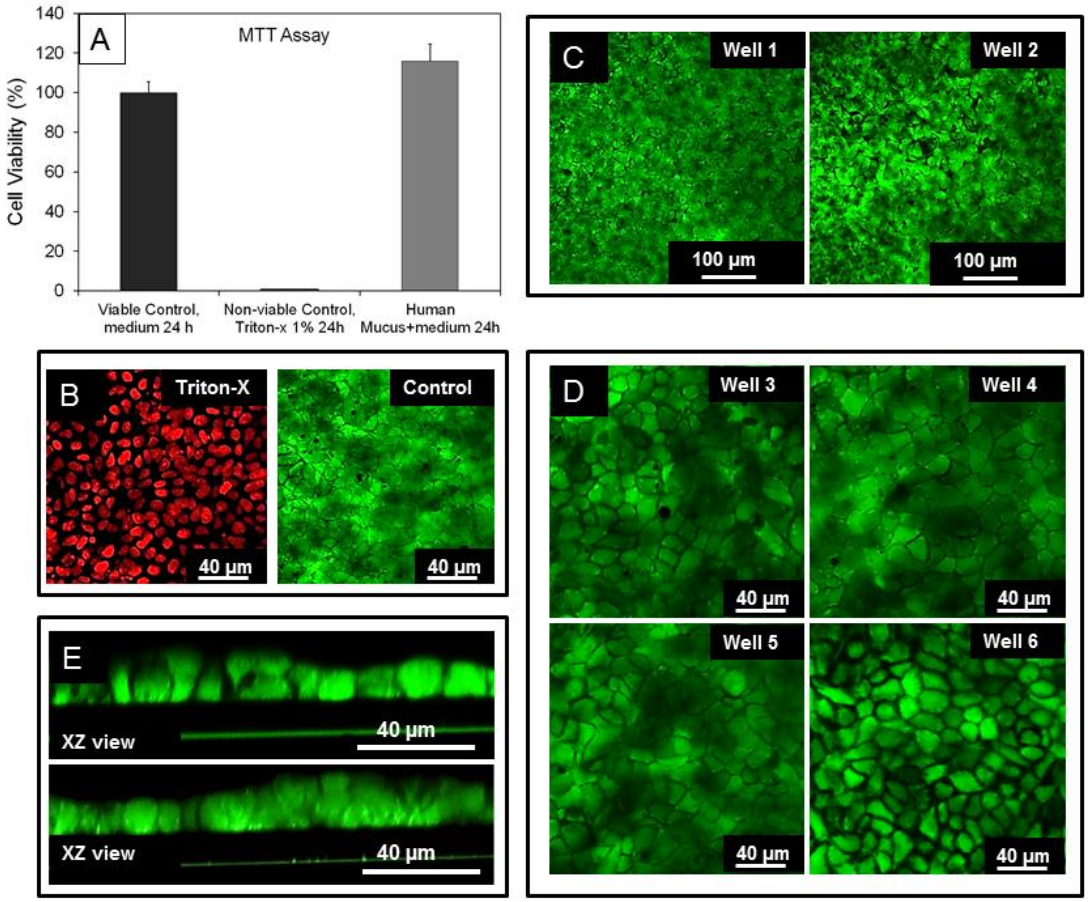

Figure 3. The viability of CFBE41o- cells upon contact with exogenous human mucus was assessed with the MTT assay and by live/dead staining with fluorescein diacetate (FDA) and propidium iodide (PI). (A) CFBE41o- cells exposed to mucus for 24 hours had a viability over 100 % (grey bar), slightly greater than that of control cells incubated with the appropriate medium (black bar); CFBE41o- cells incubated with the detergent Triton-X served as a negative control with 0% viability. (B) Representative fluorescence microphotographs of the negative (left) and positive (right) controls for the live/dead staining; cells with their nuclei stained in red represent non-viable cells, whereas cells with a green cytoplasm represent viable cells. (C) and (D) Representative fluorescence microphotographs of independent experiments at different magnifications, showing different Transwells® (wells 1-6) supporting CFBE41o- monolayers that had been incubated for 24 hours with human mucus in the apical compartment. (E) X-Z cross-sectional view of viable CFBE41o- monolayers that had been incubated for 24 hours with human mucus.

Having confirmed with two different methods the compatibility of the CFBE41o- monolayers with exogenous mucus, the next step consisted of addressing whether CFBE41o- monolayers would retain their epithelial barrier properties after adding exogenous mucus. For that purpose we indirectly assessed the presence of tight junctions by comparing the TEER values of the cells before and 24 h after coating the monolayer with mucus (Figure 4). Monolayers incubated without mucus but under the same experimental conditions were used as controls. Under both conditions the barrier properties of the CFBE41o- cell monolayers remained intact. Thus, unlike in the work of Boegh *et al*., where the TEER values dropped after adding external pig gastric mucus to Caco-2 cells (38), in the present constellation the barrier properties were maintained after mucus addition. The most plausible explanation for the compatibility between the CFBE41o- cells and the exogenous pulmonary mucus may be the common human origin of both materials. In addition, the freeze-drying process may have contributed, in combination with the antibiotics in the cell culture medium, to keep the model sterile and to maintain high cell viability and intact barrier properties. No signs of bacterial contamination were observed with the use of freeze-dried mucus.

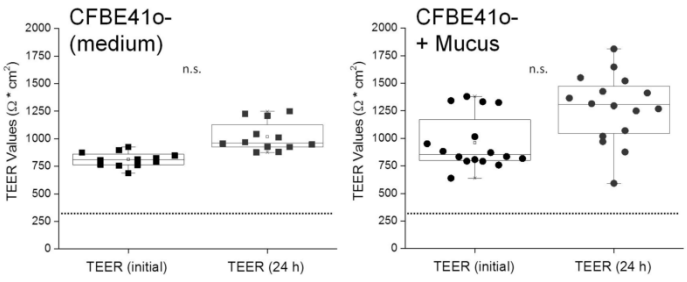

Figure 4. The barrier properties of the CFBE41o- monolayers grown for at least 10 days under submerged conditions were monitored for 24 h. The TEER values were measured before (initial) and 24 h after addition of (CFBE41o- + Mucus, right). CFBE41o-cells not exposed to mucus but incubated under submerged conditions with regular medium served as controls (CFBE41o-, left). The horizontal line at 300 Ω*cm^2 indicates the threshold values deemed to indicate the presence of a tight barrier. The mean ± SE of n=12 (CFBE41o-) and n=16 (CFBE41o- + mucus) from three independent experiments are shown. No significant (n.s.) differences were found.

3.5 Sodium fluorescein transport

The pulmonary mucus is a selective barrier that allows the permeation of small molecules such as nutrients, growth factors, and antibodies, but significantly hinders the movement of particulates with a size greater than 100-200 nm (8, 22, 23). The apical-to-basolateral transport of the small hydrophilic model drug sodium fluorescein (376.3 Da) is routinely used to assess the paracellular transport and the barrier properties of *in vitro* epithelial models (20, 40, 41). We hypothesized that sodium fluorescein is small enough to permeate through the mucus pores and would not significantly interact with the mucus fibers due to its negative charge. Therefore, one could expect a similar transport rate of the molecule through the CFBE41o- monolayers, as well as equivalent P_{app} values, in either the presence or absence of mucus. CFBE41o- monolayers, with or without mucus, were indeed observed to act similarly as a barrier to paracellular transport (Figure 5A), with both conditions resulting in P_{app} values below 1 x 10^{-6} cm/s. A slight although not significant lower extent of permeation of sodium fluorescein could however be observed in the CFBE41o- monolayers incubated with human mucus (Figure 5B), most probably due to

interactions between the compound and mucus elements in a setting of two unstirred layers of different viscosity within the first hour after sodium fluorescein addition.

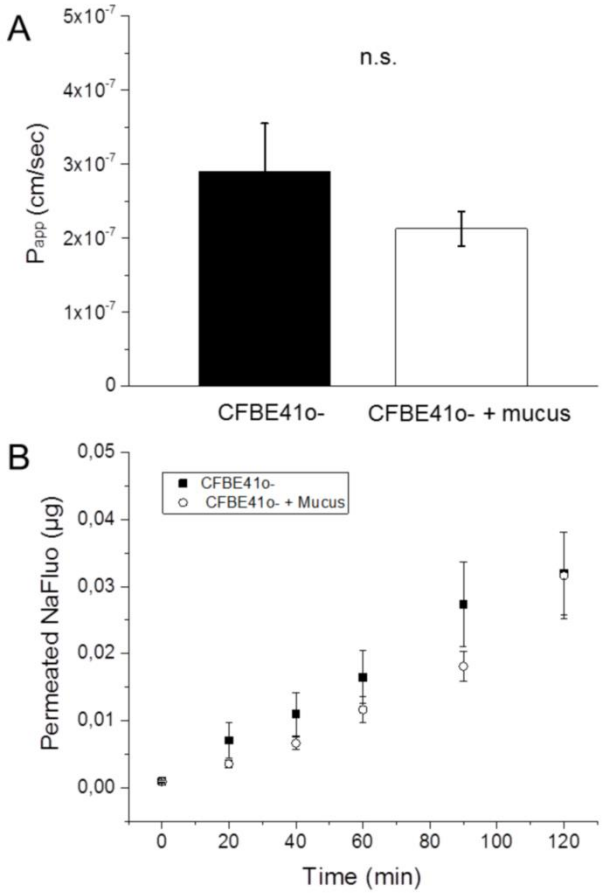

Figure 5. The barrier properties of the CFBE41o- monolayers after their exposure to mucus were determined by measuring the permeability of sodium fluorescein (NaFluo) over time. (A) Apparent permeability (P_{app}) of sodium fluorescein through CFBE41o- monolayers compared to CFBE41o- monolayers supplemented with human mucus. (B) Permeated total amount of NaFluo over time through CFBE41o- monolayers (solid squares) compared to CFBE41o- monolayers supplemented with human mucus (empty circles). The mean ± SE for n=20 from 3 independent experiments are shown. No significant (n.s.) differences were found.

3.6 Mucus is a barrier to polymeric nanoparticles

The mesh-like structure of pulmonary mucus is mainly given by a highly cross-linked mucin network (Figure 6A). The size of the pores of the mucus mesh is highly heterogeneous and ranges from very small pores of just a few nanometers to larger pores on the microscale (22, 23). Therefore, mucus represents a steric barrier to the diffusion of NPs. In addition, mucus can also filter NPs by specific chemical interactions. For instance, the sialic acid-rich glycan side-chains of the mucins confer a negative charge on mucus (42); mucins also possess non-glycosylated regions with a high capacity for hydrophobic interactions (43). As a result, a large fraction of NPs with a size above 100 nm that theoretically can chemically interact with mucus will become immobilized within the mucus mesh (3, 8, 22, 23). These findings highlight the outstanding filtering properties of pulmonary mucus against NP-based drug delivery systems. As a proof of concept for the developed *in vitro* model, we incubated chitosan coated PLGA NPs for 24 h together with "naked" CFBE41o- cell monolayers (Figure 6B), as well as with CFBE41o- cell monolayers supplemented with an additional mucus layer (Figure 6B). Thereafter we qualitatively addressed NP uptake by means of confocal microscopy.

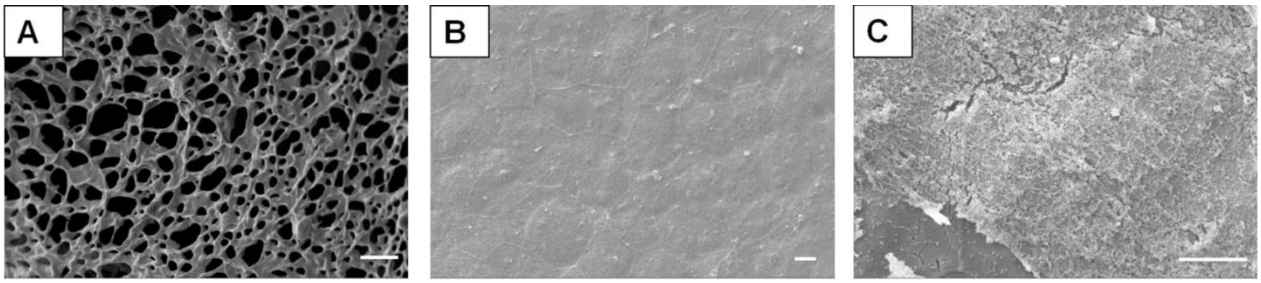

Figure 6. (A) Scanning electron microscopy (SEM) image of freeze-dried human tracheal mucus. (B) Representative SEM image of a CFBE41o- monolayer; cell boundaries between neighboring cells are visible. (C) SEM image of human tracheal mucus on top of a CFBE41o- cell monolayer; the mucus mesh structure seen in (A) is lost due to the chemical fixation. Scale bar = 4 µm.

The produced chitosan-PLGA NPs had a size of 167.8 ± 3.6 nm (PDI 0.1 ± 0.01, Figure 7) and were positively charged, as evidenced by a ζ-potential of 12.9 ± 1.9 mV.

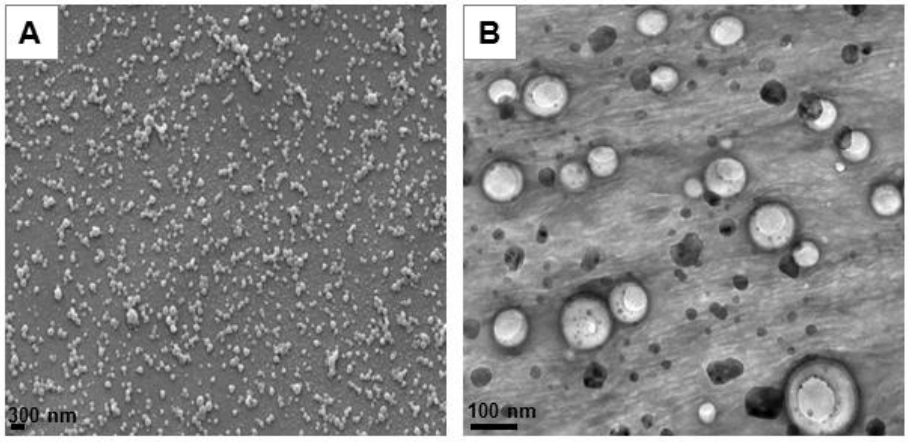

Figure 7. (A) Scanning electron microscope (SEM) and (B) transmission electron microscope (TEM) images showing the morphology of DiD labeled chitosan-PLGA nanoparticles.

This type of NPs was chosen because they have been already used for several applications of pulmonary nucleic acid delivery (44-46). Additionally, chitosan coatings have been shown to induce efficient transfection in various cell lines (27, 28), including CFBE41o- (12). We hypothesized, however, that with a NP diameter close to 200 nm and due to the known mucoadhesive properties of chitosan (47), most of the NPs would be trapped within the mucus layer, precluding their cellular uptake. When NPs were incubated with the "naked" CFBE41o- cell monolayers, a significant uptake could be observed from the confocal images (Figure 8A). On the other hand, when the chitosan-PLGA NPs were incubated with CFBE41o- monolayers that were supplemented with a layer of mucus, the number of NPs in close proximity to the cells was negligible, indicating that most of the NPs had been entrapped by the mucus layer (Figure 8B) which was itself washed away during the staining/fixation procedure. This finding further

confirmed our hypothesis, and indicates that the drug delivery efficiency of NP-based systems is dramatically reduced in mucosal tissues.

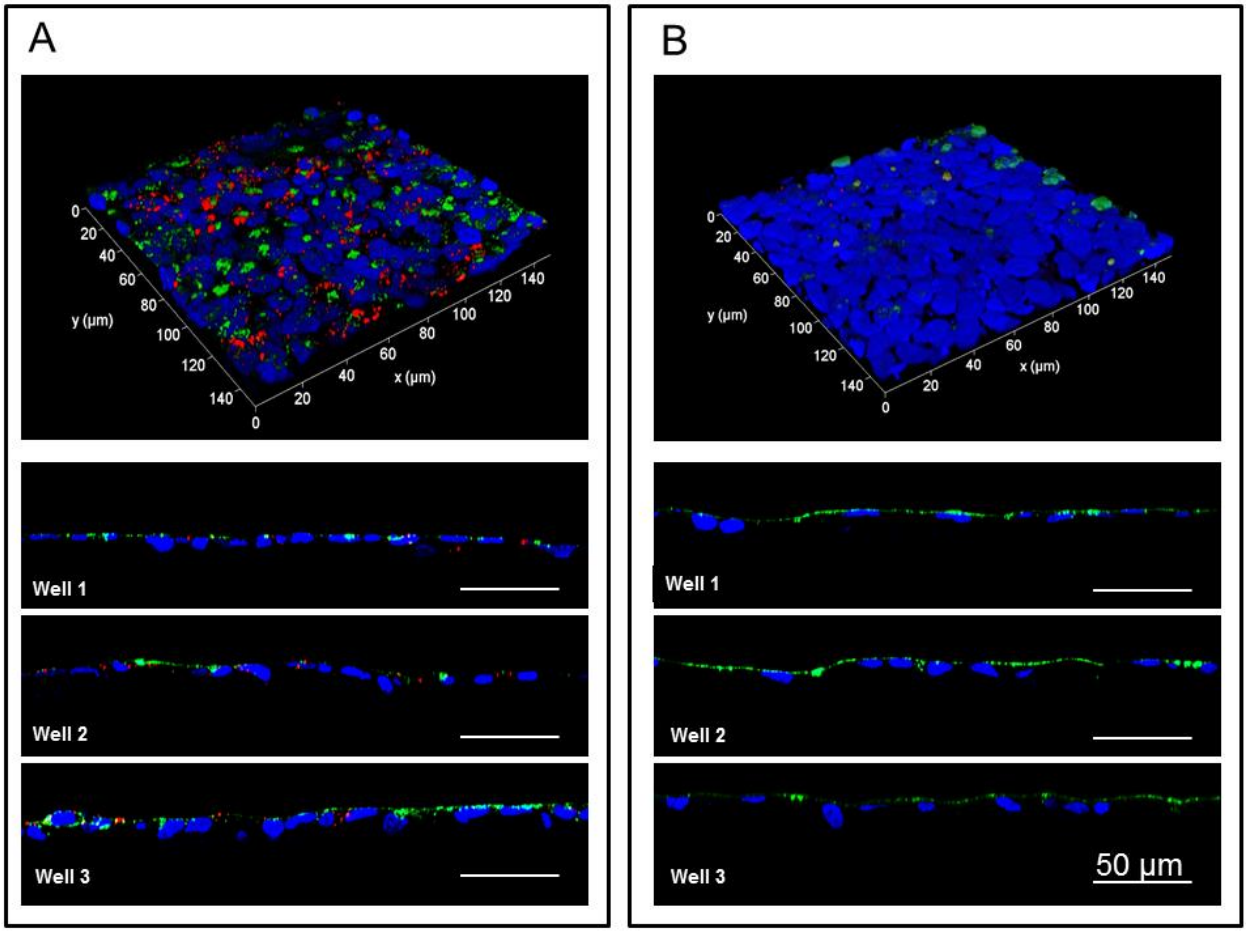

Figure 8. Confocal laser scanning microscopy images of the cellular uptake study performed with DiD-labeled chitosan-PLGA nanoparticles (NP) on CFBE41o- cells with and without mucus. (A) CFBE41o- monolayers were incubated with 400 µl of the NP suspension (40 µg/ml) for 24 h; after incubation, although the apical surface was thoroughly washed with PBS, a widespread presence of NPs either in close contact with or internalized by cells was noted, as evidenced by the 3D rendering (top) and the X-Z cross-sections (wells 1-3). (B) CFBE41o- monolayers supplemented with human tracheal mucus were incubated with 400 µl of the NP suspension (40 µg/ml) for 24 h. After incubation, the apical surface was thoroughly washed with PBS, resulting in the removal of both mucus and entrapped NPs. The absence of NPs in contact with cells in this case indicates that a vast majority of the NPs were

trapped within the mucus and washed away. Nuclei were stained with DAPI (blue), the cell membrane was stained with wheat germ agglutinin (green), and the DiD-labelled chitosan-PLGA NPs were labelled with DiD (red).

4. CONCLUSION

The aim of this work was to develop an *in vitro* model of the bronchial region comprising minimally an epithelial cell layer and a layer of pulmonary mucus. As a cellular element, we used the CF cell line CFBE41o-, which possesses a number of interesting features for pharmaceutical research such as the expression of tight junction proteins and proteins relevant for pulmonary drug transport. Nevertheless, this cell line is unable to secrete mucus, and therefore the cell monolayer alone as an *in vitro* model lacks a key protective element found in the airways *in vivo*. To complement the cell monolayer, small amounts of freeze-dried human tracheal mucus were placed on top of the CFBE41o- cells, creating an air-mucus interface. The rheological properties of the re-hydrated mucus were very similar to the native material. Moreover, the biocompatibility of the exogenous mucus with the cells could be demonstrated. The re-hydrated mucus behaved as a semi-permeable layer, allowing the small molecule sodium fluorescein to permeate but severely hindering the passage of positively-charged 168 nm diameter polymeric NPs, as evidenced by the low degree of particle uptake by CFBE41o- cells in the presence of mucus. Hence, this model combines the excellent epithelial barrier properties of CFBE41o- cells with the option to implement an additional mucus barrier. Moreover, the relatively short culture time needed to achieve a tight epithelial monolayer allows having a cell line-based mucus-containing *in vitro* model ready for experiments within a timeframe of less than a week. The model may therefore prove a useful tool to study inhalation pharmaceuticals targeted to the bronchial mucosa and in particular to address the role of mucus in this context.

ACKNOWLEDGEMENTS

The authors would like to acknowledge the excellent technical assistance of Dr Chiara de Rossi, Petra König, Peter Meiers, and Jana Westhues. This work was partly supported by the Marie Curie Initial Training Network PathChooser (PITNGA-2013-608373).

5. REFERENCES

1. Rubin BK. Physiology of airway mucus clearance. Respiratory care. 2002 Jul;47(7):761-8.

2. Ruge CA, Kirch J, Lehr CM. Pulmonary drug delivery: from generating aerosols to overcoming biological barriers-therapeutic possibilities and technological challenges. The lancet Respiratory medicine. 2013 Jul;1(5):402-13.

3. Schuster BS, Suk JS, Woodworth GF, Hanes J. Nanoparticle diffusion in respiratory mucus from humans without lung disease. Biomaterials. 2013 Apr;34(13):3439-46.

4. Antunes MB, Cohen NA. Mucociliary clearance--a critical upper airway host defense mechanism and methods of assessment. Current opinion in allergy and clinical immunology. 2007 Feb;7(1):5-10.

5. Button B, Cai LH, Ehre C, Kesimer M, Hill DB, Sheehan JK, et al. A periciliary brush promotes the lung health by separating the mucus layer from airway epithelia. Science. 2012 Aug 24;337(6097):937-41.

6. Knowles MR, Boucher RC. Mucus clearance as a primary innate defense mechanism for mammalian airways. The Journal of clinical investigation. 2002 Mar;109(5):571-7.

7. Ramos FL, Krahnke JS, Kim V. Clinical issues of mucus accumulation in COPD. International journal of chronic obstructive pulmonary disease. 2014;9:139-50.

8. Sanders NN, De Smedt SC, Van Rompaey E, Simoens P, De Baets F, Demeester J. Cystic fibrosis sputum: a barrier to the transport of nanospheres. American journal of respiratory and critical care medicine. 2000 Nov;162(5):1905-11.

9. Yuan S, Hollinger M, Lachowicz-Scroggins ME, Kerr SC, Dunican EM, Daniel BM, et al. Oxidation increases mucin polymer cross-links to stiffen airway mucus gels. Science translational medicine. 2015 Feb 25;7(276):276ra27. PubMed PMID: 25717100.

10. Innes AL, Carrington SD, Thornton DJ, Kirkham S, Rousseau K, Dougherty RH, et al. Ex vivo sputum analysis reveals impairment of protease-dependent mucus degradation by plasma proteins in acute asthma. American journal of respiratory and critical care medicine. 2009 Aug 1;180(3):203-10. PubMed PMID: 19423716.

11. Elborn JS. Cystic fibrosis. Lancet. 2016 Apr 29.

12. Fernandez Fernandez E, Santos-Carballal B, Weber WM, Goycoolea FM. Chitosan as a non-viral co-transfection system in a cystic fibrosis cell line. International journal of pharmaceutics. 2016 Apr 11;502(1-2):1-9.

13. Fields RJ, Cheng CJ, Quijano E, Weller C, Kristofik N, Duong N, et al. Surface modified poly(beta amino ester)-containing nanoparticles for plasmid DNA delivery. Journal of controlled release : official journal of the Controlled Release Society. 2012 Nov 28;164(1):41-8.

14. Bangel-Ruland N, Tomczak K, Fernandez Fernandez E, Leier G, Leciejewski B, Rudolph C, et al. Cystic fibrosis transmembrane conductance regulator-mRNA delivery: a novel alternative for cystic fibrosis gene therapy. The journal of gene medicine. 2013 Nov-Dec;15(11-12):414-26.

15. Ehrhardt C, Collnot EM, Baldes C, Becker U, Laue M, Kim KJ, et al. Towards an in vitro model of cystic fibrosis small airway epithelium: characterisation of the human bronchial epithelial cell line CFBE41o. Cell and tissue research. 2006 Mar;323(3):405-15.

16. Kong M, Maeng P, Hong J, Szczesniak R, Sorscher E, Sullender W, et al. Respiratory syncytial virus infection disrupts monolayer integrity and function in cystic fibrosis airway cells. Viruses. 2013 Sep;5(9):2260-71. PubMed PMID: 24056672.

17. Nilsson HE, Dragomir A, Lazorova L, Johannesson M, Roomans GM. CFTR and tight junctions in cultured bronchial epithelial cells. Experimental and molecular pathology. 2010 Feb;88(1):118-27.

18. Molenda N, Urbanova K, Weiser N, Kusche-Vihrog K, Gunzel D, Schillers H. Paracellular transport through healthy and cystic fibrosis bronchial epithelial cell lines--do we have a proper model? PloS one. 2014;9(6):e100621.

19. Grainger CI, Greenwell LL, Lockley DJ, Martin GP, Forbes B. Culture of Calu-3 cells at the air interface provides a representative model of the airway epithelial barrier. Pharmaceutical research. 2006 Jul;23(7):1482-90.

20. Haghi M, Young PM, Traini D, Jaiswal R, Gong J, Bebawy M. Time- and passage-dependent characteristics of a Calu-3 respiratory epithelial cell model. Drug development and industrial pharmacy. 2010 Oct;36(10):1207-14.

21. Mura S, Hillaireau H, Nicolas J, Kerdine-Romer S, Le Droumaguet B, Delomenie C, et al. Biodegradable nanoparticles meet the bronchial airway barrier: how surface properties affect their interaction with mucus and epithelial cells. Biomacromolecules. 2011 Nov 14;12(11):4136-43.

22. Murgia X, Pawelzyk P, Schaefer UF, Wagner C, Willenbacher N, Lehr CM. Size-Limited Penetration of Nanoparticles into Porcine Respiratory Mucus after Aerosol Deposition. Biomacromolecules. 2016 Apr 11;17(4):1536-42.

23. Kirch J, Schneider A, Abou B, Hopf A, Schaefer UF, Schneider M, et al. Optical tweezers reveal relationship between microstructure and nanoparticle penetration of pulmonary mucus. Proceedings of the National Academy of Sciences of the United States of America. 2012 Nov 6;109(45):18355-60.

24. Patton JS, Brain JD, Davies LA, Fiegel J, Gumbleton M, Kim KJ, et al. The particle has landed--characterizing the fate of inhaled pharmaceuticals. Journal of aerosol medicine and pulmonary drug delivery. 2010 Dec;23 Suppl 2:S71-87.

25. Sigurdsson HH, Kirch J, Lehr CM. Mucus as a barrier to lipophilic drugs. International journal of pharmaceutics. 2013 Aug 30;453(1):56-64.

26. Yang X, Forier K, Steukers L, Van Vlierberghe S, Dubruel P, Braeckmans K, et al. Immobilization of pseudorabies virus in porcine tracheal respiratory mucus revealed by single particle tracking. PloS one. 2012;7(12):e51054.

27. Csaba N, Koping-Hoggard M, Alonso MJ. Ionically crosslinked chitosan/tripolyphosphate nanoparticles for oligonucleotide and plasmid DNA delivery. International journal of pharmaceutics. 2009 Dec 1;382(1-2):205-14.

28. Mao HQ, Roy K, Troung-Le VL, Janes KA, Lin KY, Wang Y, et al. Chitosan-DNA nanoparticles as gene carriers: synthesis, characterization and transfection efficiency. Journal of controlled release : official journal of the Controlled Release Society. 2001 Feb 23;70(3):399-421.

29. Thomas M, Klibanov AM. Non-viral gene therapy: polycation-mediated DNA delivery. Applied microbiology and biotechnology. 2003 Jul;62(1):27-34.

30. Rubin BK, Finegan B, Ramirez O, King M. General anesthesia does not alter the viscoelastic or transport properties of human respiratory mucus. Chest. 1990 Jul;98(1):101-4.

31. Rubin BK, Ramirez O, Zayas JG, Finegan B, King M. Collection and analysis of respiratory mucus from subjects without lung disease. The American review of respiratory disease. 1990 Apr;141(4 Pt 1):1040-3.

32. Nafee N, Schneider M, Schaefer UF, Lehr CM. Relevance of the colloidal stability of chitosan/PLGA nanoparticles on their cytotoxicity profile. International journal of pharmaceutics. 2009 Nov 3;381(2):130-9.

33. Sporty JL, Horalkova L, Ehrhardt C. In vitro cell culture models for the assessment of pulmonary drug disposition. Expert opinion on drug metabolism & toxicology. 2008 Apr;4(4):333-45.

34. Kreft ME, Jerman UD, Lasic E, Lanisnik Rizner T, Hevir-Kene N, Peternel L, et al. The characterization of the human nasal epithelial cell line RPMI 2650 under different culture conditions and their optimization for an appropriate in vitro nasal model. Pharmaceutical research. 2015 Feb;32(2):665-79.

35. Loman S, Radl J, Jansen HM, Out TA, Lutter R. Vectorial transcytosis of dimeric IgA by the Calu-3 human lung epithelial cell line: upregulation by IFN-gamma. The American journal of physiology. 1997 May;272(5 Pt 1):L951-8.

36. Ehrhardt C, Fiegel J, Fuchs S, Abu-Dahab R, Schaefer UF, Hanes J, et al. Drug absorption by the respiratory mucosa: cell culture models and particulate drug carriers. Journal of aerosol medicine : the official journal of the International Society for Aerosols in Medicine. 2002 Summer;15(2):131-9.

37. Zayas JG, Man GC, King M. Tracheal mucus rheology in patients undergoing diagnostic bronchoscopy. Interrelations with smoking and cancer. The American review of respiratory disease. 1990 May;141(5 Pt 1):1107-13.

38. Boegh M, Baldursdottir SG, Mullertz A, Nielsen HM. Property profiling of biosimilar mucus in a novel mucus-containing in vitro model for assessment of intestinal drug absorption. European journal of pharmaceutics and biopharmaceutics : official journal of Arbeitsgemeinschaft fur Pharmazeutische Verfahrenstechnik eV. 2014 Jul;87(2):227-35.

39. Teubl BJ, Absenger M, Frohlich E, Leitinger G, Zimmer A, Roblegg E. The oral cavity as a biological barrier system: design of an advanced buccal in vitro permeability model. European

journal of pharmaceutics and biopharmaceutics : official journal of Arbeitsgemeinschaft fur Pharmazeutische Verfahrenstechnik eV. 2013 Jun;84(2):386-93.

40. Kuehn A, Kletting S, de Souza Carvalho-Wodarz C, Repnik U, Griffiths G, Fischer U, et al. Human alveolar epithelial cells expressing tight junctions to model the air-blood barrier. Altex. 2016;33(3):251-60.

41. Hermanns MI, Unger RE, Kehe K, Peters K, Kirkpatrick CJ. Lung epithelial cell lines in coculture with human pulmonary microvascular endothelial cells: development of an alveolo-capillary barrier in vitro. Laboratory investigation; a journal of technical methods and pathology. 2004 Jun;84(6):736-52.

42. Ludwig A. The use of mucoadhesive polymers in ocular drug delivery. Advanced drug delivery reviews. 2005 Nov 3;57(11):1595-639.

43. Lai SK, Wang YY, Hanes J. Mucus-penetrating nanoparticles for drug and gene delivery to mucosal tissues. Advanced drug delivery reviews. 2009 Feb 27;61(2):158-71.

44. Mahiny AJ, Dewerth A, Mays LE, Alkhaled M, Mothes B, Malaeksefat E, et al. In vivo genome editing using nuclease-encoding mRNA corrects SP-B deficiency. Nature biotechnology. 2015 Jun;33(6):584-6.

45. Ravi Kumar MN, Bakowsky U, Lehr CM. Preparation and characterization of cationic PLGA nanospheres as DNA carriers. Biomaterials. 2004 May;25(10):1771-7.

46. Beisner J, Dong M, Taetz S, Nafee N, Griese EU, Schaefer U, et al. Nanoparticle mediated delivery of 2'-O-methyl-RNA leads to efficient telomerase inhibition and telomere shortening in human lung cancer cells. Lung cancer. 2010 Jun;68(3):346-54.

47. Dhawan S, Singla AK, Sinha VR. Evaluation of mucoadhesive properties of chitosan microspheres prepared by different methods. AAPS PharmSciTech. 2004;5(4):e67.